Title: On the reproductive mechanism of Gram-negative protocells

Dheeraj Kanaparthi[1,2&3*], Marko Lampe[4], Baoli Zhu[2&5], Andreas Klingl[6], Tillmann Lueders[2&3*] & Petra Schwille[1*]

Affiliations:

[1]Max-Planck Institute for Biochemistry, Munich, Germany

[2]Chair of Ecological Microbiology, BayCeer, University of Bayreuth, Germany.

[3]Helmholtz Center Munich, Germany.

[4]Advanced Light Microscopy Facility, European Molecular Biology Laboratory, Heidelberg, Germany.

[5]Key Laboratory of Agro-ecological Processes in Subtropical Regions, Taoyuan Agroecosystem Research Station, Institute of Subtropical Agriculture, Chinese Academy of Sciences, Changsha, China.

[6]Department of Biology, LMU, Planegg-Martinsried, Germany.

Abstract: Protocells are thought to have existed on early Earth before the origin of prokaryotes. These primitive cells are believed to have carried out processes like replication solely based on the physicochemical properties of their cell constituents. Despite considerable efforts, replication of a living cell-driven entirely by laws of physics and chemistry has never been achieved. To test this hypothesis, we transformed extant bacteria into sacks of cytoplasm, incapable of regulating either their morphology or reproductive processes. We then exposed these proxy-protocells (bacterial protoplasts) to presumed Archaean Eon environmental conditions to understand if or how these cells reproduce. Contrary to the current presumption that bacterial protoplasts reproduce in a haphazard manner, under our experimental conditions they reproduced via a multi-stage reproductive cycle, resulting in viable daughter cells. Our observations suggest that this mechanism of reproduction could in fact be well explained from a biophysical perspective. Based on our observations we argue that this method of reproduction is better suited for the environmental conditions of early Earth.

Graphical abstract:

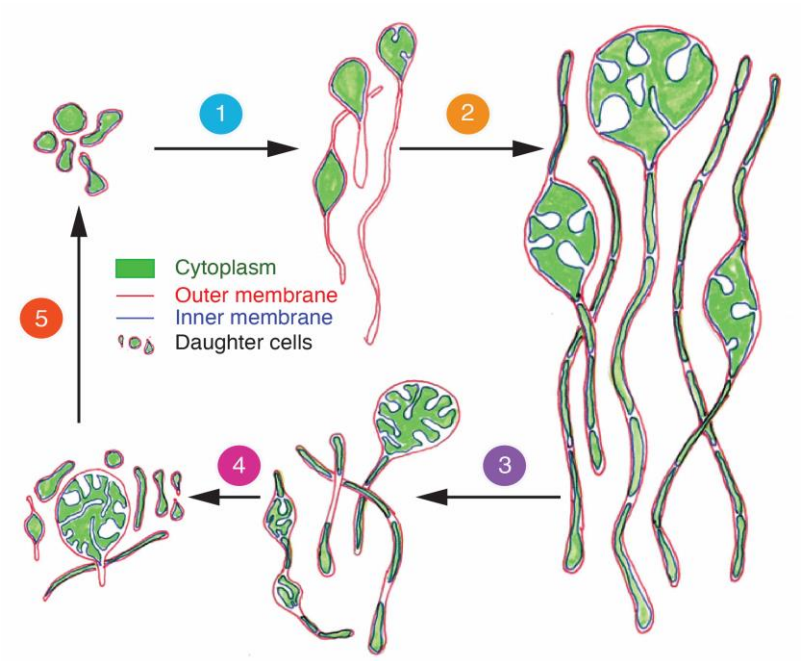

INTRODUCTION: Normal functioning of a cell, like maintaining consistent morphology and replication are mechanistically complex processes requiring co-ordination between multitude of enzymes and structural proteins [1,2]. With an increasing structural and organizational complexity of organisms (from prokaryotes to eukaryotes), such process becomes even more complex [3,4]. Over the past few decades, considerable progress has been made in our understanding of how complexity in biological processes evolved from prokaryotes to eukaryotes [5]; however, origin of these processes in prokaryotes from even simpler life forms remains a far less understood process. Theory of chemical evolution [6] proposes that, prokaryotes evolved from more primitive protocells [7]. These cells are thought to be devoid of all molecular biological mechanisms and were dependent on physicochemical properties of their cell constituents for mediating important cellular processes like replication [8]. Despite being a key evolutionary link between abiotic chemical reactions on early Earth and prokaryotes, protocells to date remained a theoretical possibility with no definitive proof for their existence on early Earth, nor was it demonstrated that physicochemical forces alone could mediate complex biological processes like cell division. In the present study we attempted to understand protocell reproductive process and test the possibility if processes like cell replication could be entirely mediated by physiochemical properties of cell constituents, using bacterial protoplasts as proxy-protocells.

Like protocells, bacteria in their protoplast state are incapable of either regulating their morphology or reproductive process according to the information encoded in their genome [9]. These cells are thought to reproduce in a un-regulated and haphazard manner [10]. To understand physiochemical mechanism and evolutionary significance of this method of reproduction, here we worked with protoplasts of Gram-negative bacteria, *R. sphaeroides* (*RS-P*). Given such primitive cells could have existed on early Earth, prior to the origin of

prokaryotes and physicochemical properties of cell constituents are dependent on environmental conditions [11], we grew these protoplasts under environmental conditions of early Earth [12] to understand if and how these cells grow and reproduce.

Recent studies demonstrated that surface temperatures of Archaean Earth (4000-2500 million years ago) ranged between 26° to 35°C [13,14] and Archaean Eon Ocean were 1.5 to 2 times more saltier than the current oceans [12]. To replicate these conditions, we grew *R. sphaeroides* in half strength nutrient broth (NB) supplemented with 5-10% Dead Sea salt (DSS) at 30°C. DSS was used in our incubations rather than pure NaCl to replicate complex salt composition of Archaean oceans. We subsequently transformed *R. sphaeroides* into its protoplast (*RS-P*) state according to the procedure described in the methods section. Ones we achieved a stable protoplast, we transferred *RS-P* in fresh media and monitored its growth and morphological transformation at regular intervals. Rather than reproducing by binary fission, like in its native form or by randomly increasing in size and bursting into smaller daughter cells, as expected for protoplasts[10], in our incubations *RS-P* exhibited a very defined multi-stage life cycle. In the below sections of the manuscript, we present an in-depth morphological transformation of *RS-P*, followed by an explanation of the physicochemical mechanisms driving such transformations.

Results:

Over the course of its growth, *RS-P* went through a series of morphological transformations leading to the formation of viable daughter cells. A simplistic version of its life cycle is presented in Figure 1.

During the lag phase, growth was restricted to the outer membrane (OM) of the cell. OM grew into a hollow filamentous extension, resulting in a sperm cell like morphology (Figure 1B, 1C & Figure S1A) or spherical cells with enlarged periplasmic space (Figure S2 & Movie S1). Length of these OM extensions varied from cell-to-cell, ranging between 0.5 to 5 μm (Figure 1B, 1C & Figure S1A). Subsequently, cytoplasmic volume of the cell gradually increased, filling in the hollow template created by the peri-plasmic space (Figure 1C-D & Figure S1A, B, E & G), resulting in the formation of tubular cells (Figure 1D-G & Figure 2).

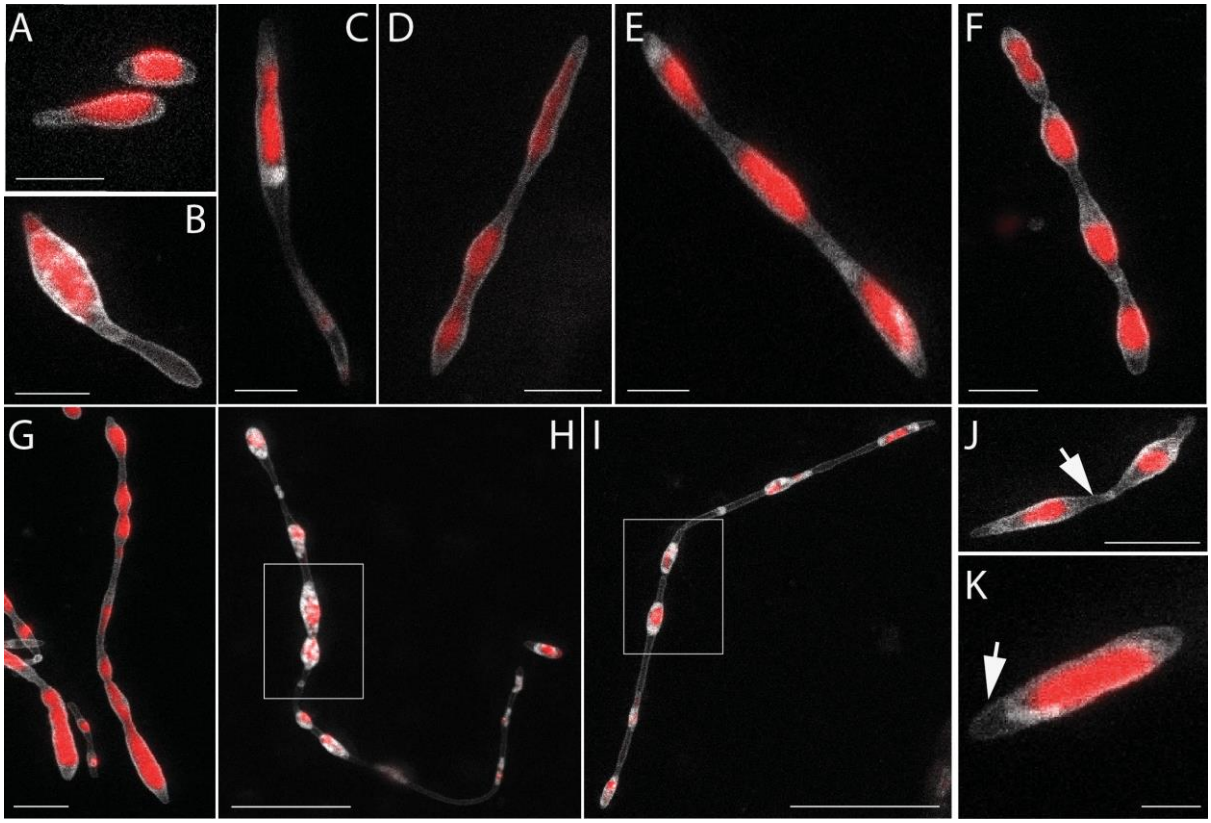

Figure 1. Life cycle of filamentous *RS-P* cells.

STED microscope Images (A-K) show life cycle of tubular and filamentous *RS-P*. Cells in these images were stained with universal membrane stain, FM™5-95 (white) and DNA stain, PicoGreen™ (red). Arrows in images J points to collapsed hollow membrane, between the cytoplasmic compartments (daughter cells). Boxes in images H&I show cytoplasmic compartments within the cell undergoing binary fission. Arrows in images K points to

remnants of such excess membrane in daughter cells. Scale bars: 1μm (A-G, I & J) and 10μm (H & I).

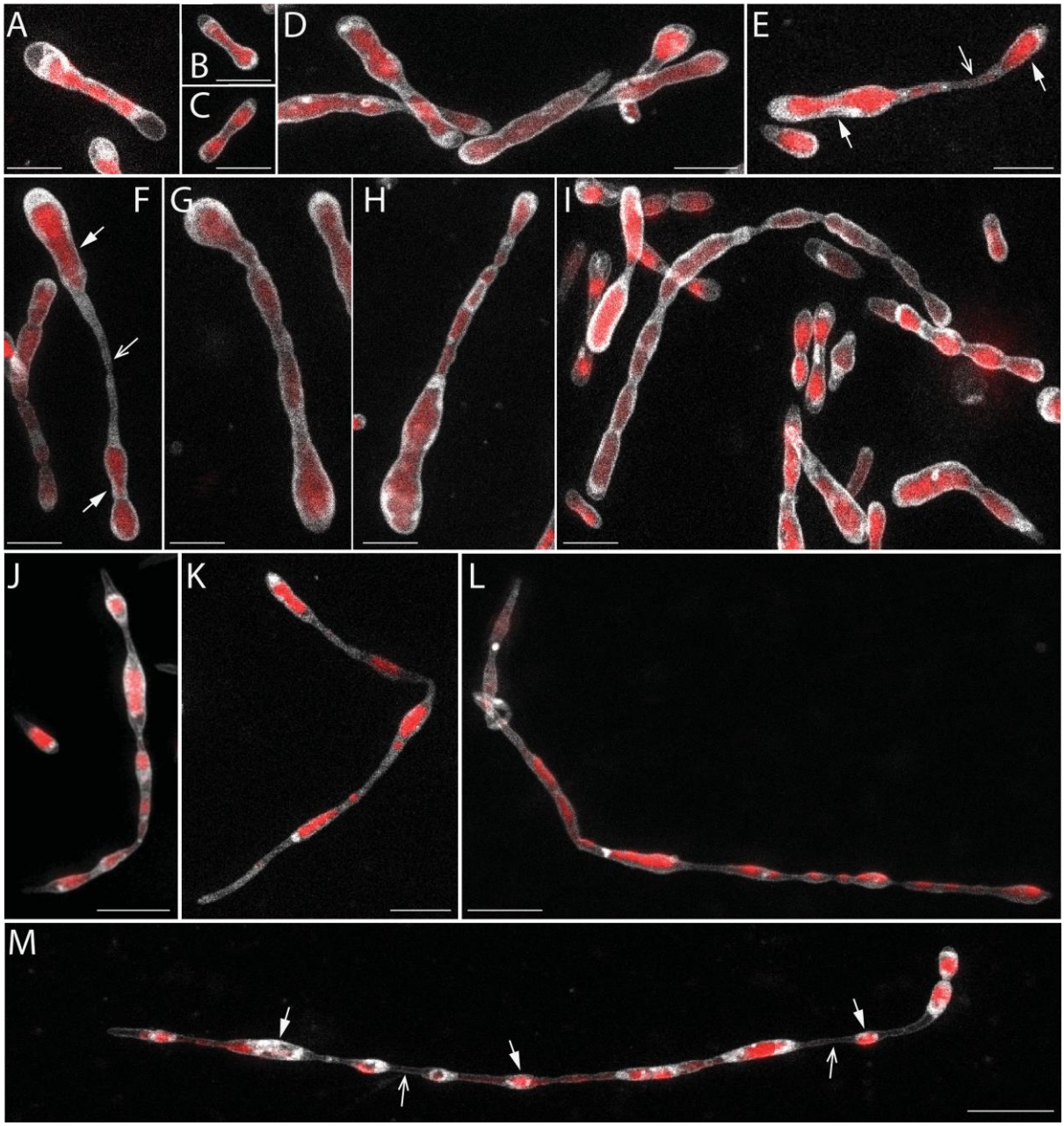

Figure 2. *RS-P*'s morphologies during log and stationary growth phase

STED microscope Images (A-M) show life cycle of tubular and filamentous *RS-P*. Cells were stained, and color coded as described in Figure 1. Images A-C show lag phase *RS-P* cells. Images D-I show log and early stationary phase *RS-P* cells. Images J-M show stationary

phase *RS-P* cells. Images E&F show dumbbell shaped cells, with arrows pointing either to dumbbell (closed arrows) and hollow OM connecting these dumbbells (open arrows). Arrows in image M points to cytoplasmic compartment enclosed in inner cell membrane (closed) and hollow OM. Scale bars: 1μm (A-I) and 5μm (J-M).

During this cytoplasmic expansion, most cells formed hollow intracellular vesicles (Figure S1D-G). These vesicles initially appeared as small buds attached to inner cell membrane followed by their expansion into or out of the cytoplasm (into the peri-plasmic space) (Figure S1E-G). No specific pattern was observed in size, number, or organization of these vesicles (Figure S1), indicating that they are not formed by a predetermined biological mechanism.

In the log phase of growth, cells underwent a significant morphological diversification. While some cells retained their tubular morphology, others developed surface depressions along their length resembling tubular vesicles subjected to curvature-induced destabilization at their surface (like Rayleigh-Plateau instability) (Figure 1D-G, 2 & S1C&D). These surface depressions were formed as a result of cytoplasmic compartment surrounded by the inner cell membrane undergoing binary fission (Figure 1 D-I). In some filamentous cells we observed cytoplasmic compartments undergoing a symmetric division leading to the formation of daughter cells of equal size (Figure 1E & F). In such cells surface depressions are uniform in size and regularly spaced. Alternately, some cells developed unevenly sized depressions with a large lenticular structure either at the tip (Figure 2F-H & 3, Figure S1B-D) or center of the filament (Figure 3A, arrow). Such structures were formed due to asymmetric division of cytoplasmic compartments (Figure S3C&D). Despite repeated attempts no uniformity was observed either in the thickness of the filaments or a pattern of surface depressions (Figure 2&3). Over time these surface depressions grew in depth and the cytoplasmic daughter

compartments were linked to each other only by the hollow outer membrane (boxed regions in Figure 1H & open arrows in Figure 2M). Subsequent rupture of hollow outer membrane led to the formation of individual daughter cells (Figure 1J, closed arrows). We also observed some tubular cell undergoing stretching to form thin filamentous cells (Figure S3).

During the stationary growth stage (after a 10-20 days of culturing), we observed cells exhibiting a mix of all above discussed morphologies (Figure 3 & S4) – individual daughter

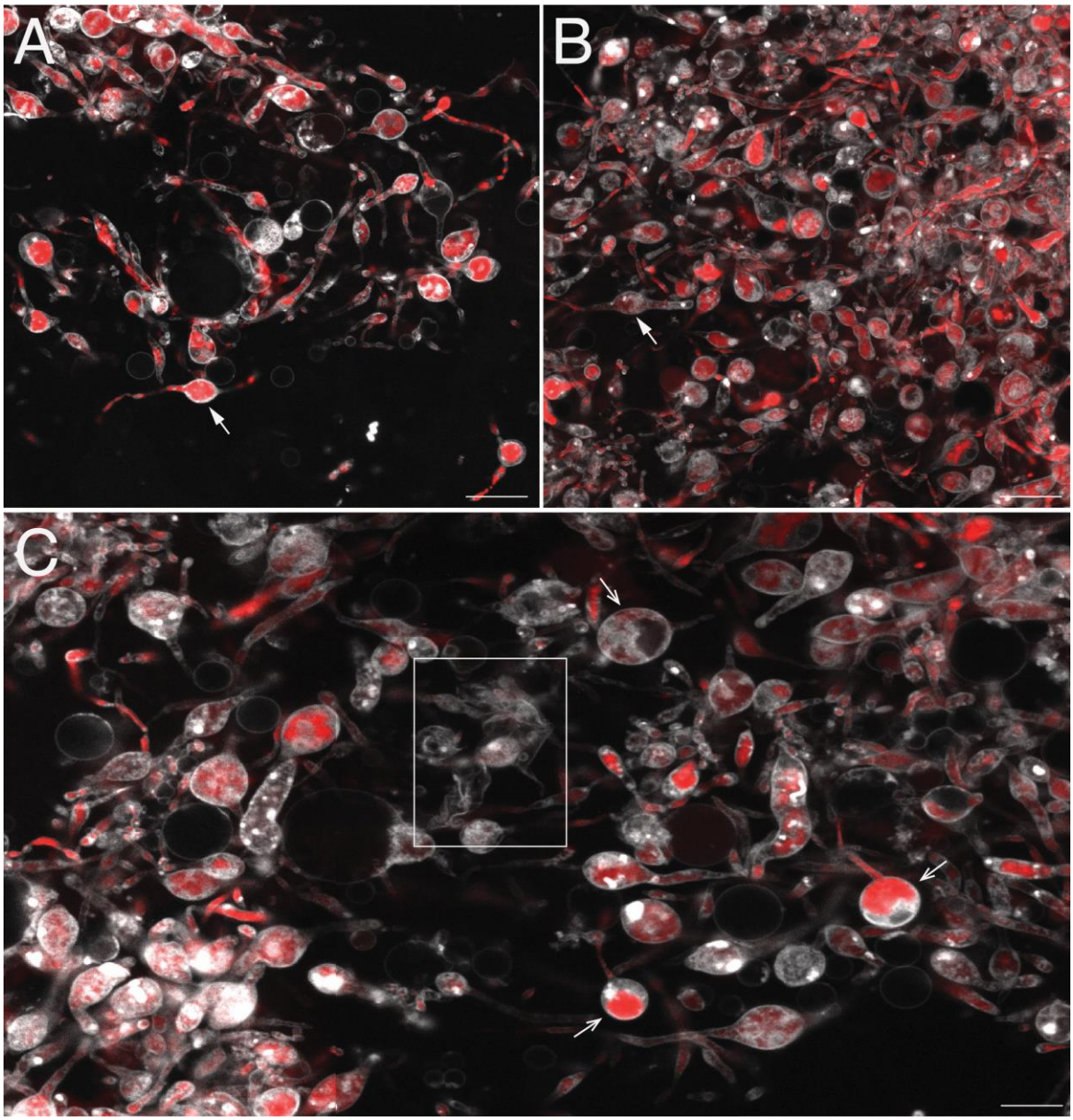

Figure 3. Lenticular *RS-P* cells with internal reticulate structures

Images A-C show *RS-P* cells in their stationary growth stage. Images show lenticular cells within the filamentous extensions either at one (open arrows) or both ends (closed arrows). Most lenticular cells contain intracellular membrane vesicles, giving them a reticulate appearance (Figure S1E-G). Cells were stained, and color coded as described in Figure 1. Scale bars: 10μm.

cells, tubular and filamentous cells, filamentous cells with lenticular structures present either at the tips or in the middle of the filaments. Most tubular and lenticular cells developed a spotted or a reticulate appearance (Figure 3 & S4), due to the accumulation of intracellular vesicles. A higher abundance of lenticular cells with sparsely distributed cytoplasm (Figure 3 & S4) were observed in this stage, possibly because these structures did not undergo cell division. In addition, considerable amount of membrane debris (Figure 3 & S4) was also observed during the stationary growth phase.

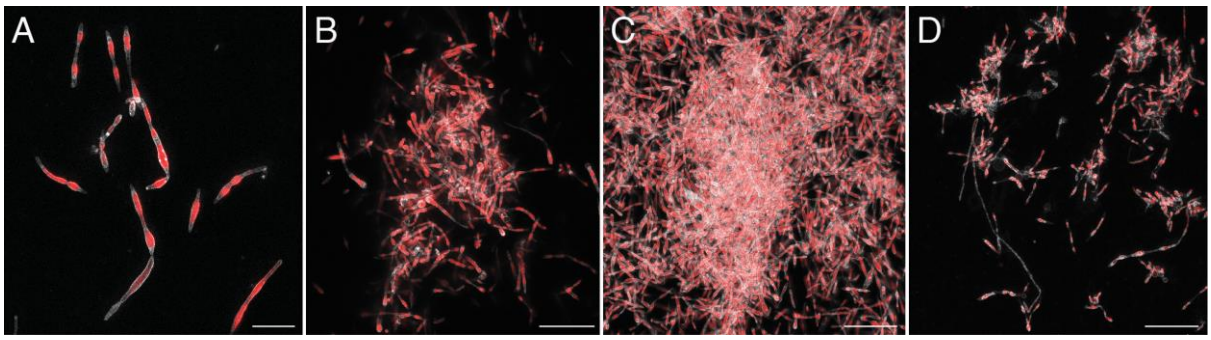

Figure 4. Morphologies of *RS-P* cells grown in NB-6%$MgCl_2$

Images A-D show *RS-P* cells of different growth stages when grown in media containing 6% $MgCl_2$ amended NB. Cells were stained, and color coded as described in Figure 1. Scale bars: 1μm (A) and 10μm (C-D).

To emulate Archaean Eon Ocean salinities, we grew *RS-P* in 7% Dead Sea salt (DSS) amended nutrient broth in all the above experiments. Different cations are known to interact differently with biological compounds and are known to alter their physical properties [15]. Hence in the subsequent experiments we attempted to understand if the morphological diversity exhibited by *RS-P* during log and stationary growth phases was due to complex salt composition of DSS. To test this possibility, we repeated the above experiments replacing DSS with equivalent concentration of divalent and monovalent cationic salts like $MgCl_2$ or KCl. When grown in the presence of KCl alone, *RS-P* exhibited morphologies and reproduced by processes very similar to the ones observed when grown with DSS (Figure S5); with the exception of forming thicker and longer filaments and comparatively bigger lenticular structures (Figure S5).

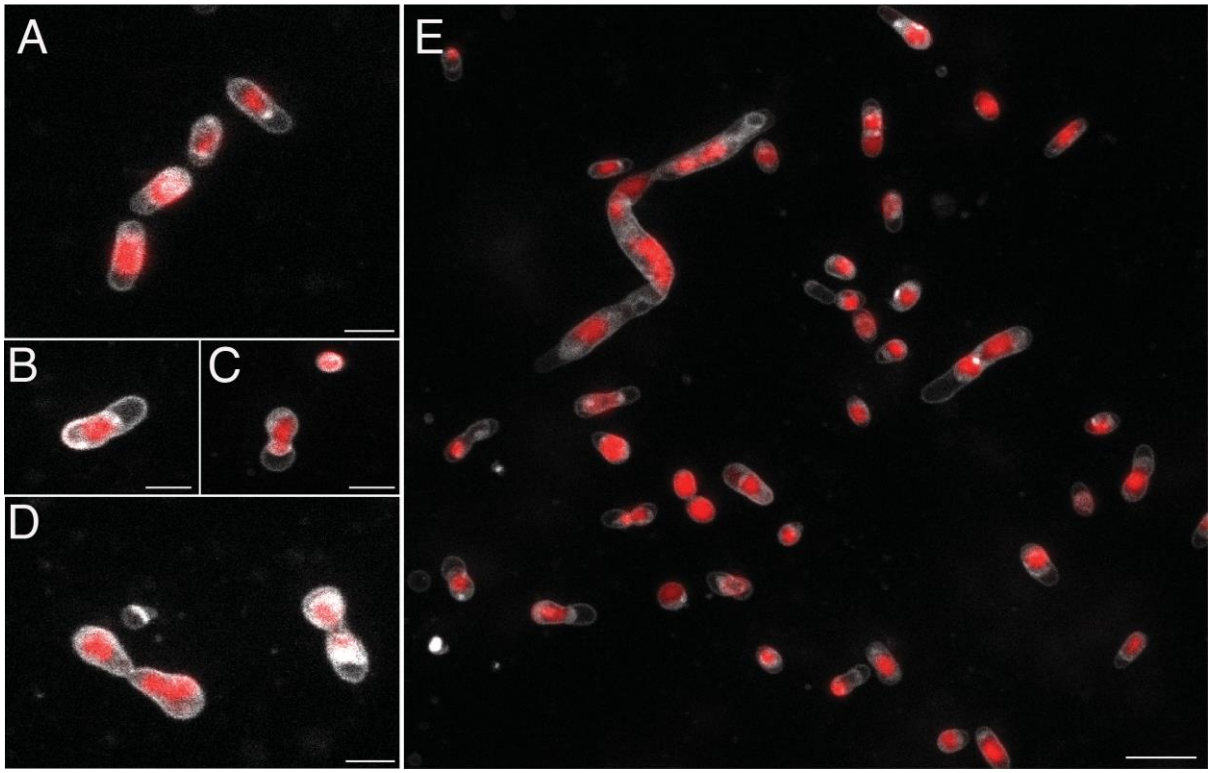

Figure 5. Morphological transformation of *RS-P* when grown on an orbital shaker

Images A-E are STED microscope images of *RS-P*. Cells were stained, and color coded as described in Figure 1. Scale bars: 2μm(A-D), 5μm (E).

Similar cell morphologies were also observed when *RS-P* was grown in $MgCl_2$, with the exception that cell sizes were considerably smaller (Figure 4 & Figure S6). Most cells observed in these incubations were of thin filamentous morphology, thick tubular cells or lenticular cells with diameter >1-2μm were rarely observed (sometimes only transiently during the mid-growth stages) (Figure 4 & Figure S6). Unlike when grown in DSS or KCl, cells observed in their last growth stage were mostly uniform in their morphology (Figure S6). Cells of this stage are predominantly unicellular daughter cells or cells in dyad undergoing binary fission. Fewer filamentous cells and even less membrane debris was observed in these incubations compared to cells when grown in DSS or KCl (Figure S6). When *RS-P* was transferred between growth media containing different salt compositions, morphologies of *RS-P* changed reversibly. This suggests that salt composition of the media determined the morphology of cells rather than the molecular biological processes within the cell.

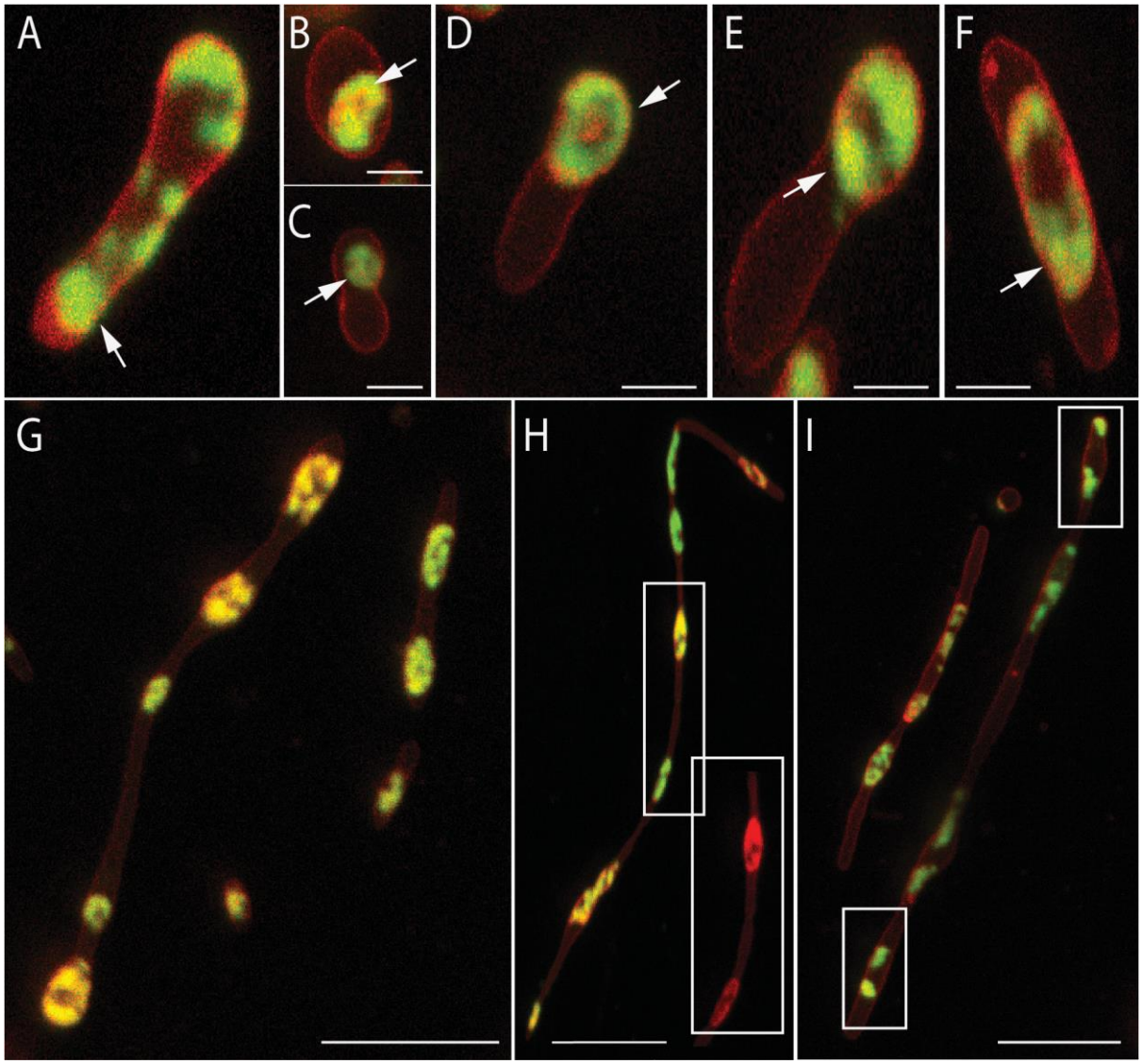

Figure 6. Membrane phase-separation in *RS-P* cells over the course of its growth

STED microscope images A-I show *RS-P* cells of different growth stages. Cells in these images were stained with universal membrane stain, FM™5-95 (red) and membrane stain that specifically stains L_d membrane, *FAST*™ Dil (green). Insert in H show the region of the filament only in FM™5-95 channel. Cytoplasmic compartment in these cells is uniformly enclosed by L_d membrane. Boxed regions in image I show cytoplasmic compartments enclosed by inner cell membrane. L_d membrane within these compartments is localized at the poles, like seen in image F. Scale bars: 1μm (A) and 10μm (C-D).

All the cultures reported above were grown under static conditions. Given such conditions are rarely encountered in natural environments, we repeated the above experiments under multiaxial elongational flow conditions by growing *RS-P* on an orbital shaker. Under these growth conditions, cells exhibited a more uniform morphology irrespective of the nature of the salt (Figure 5). Little morphological variation was observed during different growth stages. Most cells during lag, log and stationary growth stages were either individual cells or cells in dyad undergoing binary fission. Other cell morphologies or membrane debris was rarely observed.

Discussion:

Repertoire of morphologies exhibited by *RS-P* could be explained by the biophysical properties of its cell constituents and an unorderly molecular biological regulatory mechanism[9]. A similar case of malfunctioning molecular biological processes involved in mediating cell division, regulation of genes involved in maintaining internal redox state and lipid synthesis among protoplasts was reported earlier [9,16,17]. Lack of co-ordination in molecular biological processes in *RS-P* is evident from excessive lipid synthesis, leading to the formation of hollow membrane extensions (Figure 1 & S1). Based on our observations we propose a two-step process by which the hollow membrane extensions were formed. In the first step, disproportionately high lipid synthesis in comparison to cytoplasmic volume increase facilitated the transformation of excess membrane into hollow buds[18] extending either into or out of the cell (into the periplasmic space) (Figure S1G). Subsequently hollow vesicles within the periplasmic space were incorporated into the outer membrane, leading to the formation of hollow filamentous extensions (Figure 1B & Figure S1 A & E, arrow).

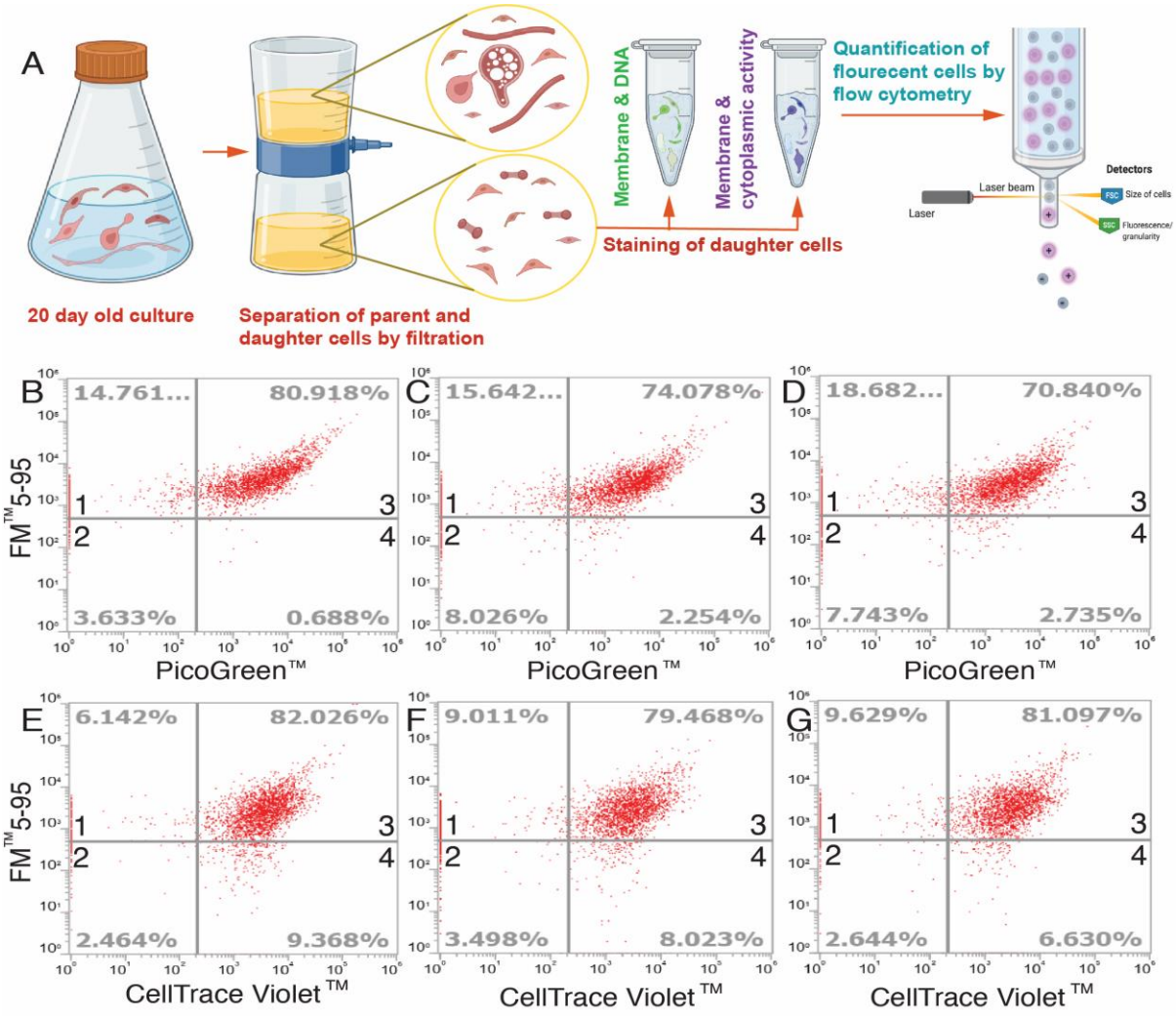

Figure 7. Viability of *RS-P* daughter cells

Panel A show the workflow of the experiment. Images B-G show flowcytometry plots. Quadrants 1, 2, 3 & 4 in each plot represent the percentage of cells stained with only FM™5-95 (1), cells stained only with PicoGreen™ (2), cells stained by both FM™5-95 & PicoGreen™ (3) and cells that were not stained either by FM™5-95 & PicoGreen™ (4). Images B-D show triplicate plots of *RS-P* cells grown in 5% -DSS-TSB and images E-G show triplicate plots of *RS-P* cells grown in 5% $MgCl_2$-TSB.

Subsequent morphologies and membrane phase-separation (Figure 6) observed in *RS-P* can be explained by the Area differential elasticity (ADE) theory [19,20]. ADE theory states that

when the area of the vesicle is smaller than that of the expected value, vesicles undergo shape deformation, leading to a series of morphological transformations. Amount of excess membrane area and intrinsic area difference (i.e., area difference between the expected and the actual area of the vesicle), determine the vesicle morphology.

As predicted by ADE model [19,20], spherical *RS-P* cells transformed in sequence from prolate shape, into a cylindrical or a dumbbell shapes and finally into "string of beads" like morphologies (Figure 1&2). Staining *RS-P* with dyes specific for fluid (L_d) and universal membrane dyes showed that, this morphological transformation was accompanied by membrane phase-separation, as proposed by ADE theory [21]. The distribution of L_o & L_d membrane observed in *RS-P* can be explained by organizational principles leading towards a stable and lowest free energy state. During early growth stages, cell membrane underwent phase-separation with L_d regions forming small patches within the cell membrane (Figure 6A). In the subsequent growth stages L_d membrane coalesced around the cytoplasmic compartment and the outer membrane in these cells was largely composed of L_o-membrane (Figure 7). In cells of subsequent growth stages and cells undergoing binary fission, presence of L_d-membrane was restricted to the poles (Figure 6 E & F), where membrane experiences a high spontaneous curvature. On the other hand, linear central barrel connecting the poles was noticed to be composed of L_o membrane (Figure 6 E & F).

Along with ADE model, morphologies of *RS-P* can also be explained from the prospective of fluid mechanics [22–24]. Growth of the cytoplasmic compartment gradually filling in the void left by outer membrane resembles the vesicle stretching under extensional flow (Figure S7). Morphological transformation of vesicles undergoing such stretching was shown be dependent on the expansional strain and elasticity of their membranes. Vesicles experiencing

a low elongational strain are shown to transformed into prolate or tubular shapes [25]. However, at a certain strain level (threshold strain), vesicles transformed into a dumbbell morphology. Any further increase in the strain, vesicles formed elongated dumbbells with beaded structures appearing along its length. Morphologies of *RS-P* observed in our study could be explained by similar physical properties like strain on the cell membrane during cytoplasmic expansion (i.e., growth) (Figure S7). High and low elongational strains on the membrane translate into high and low growth rates. In accordance with our presumption, short prolate or tubular cells were most frequently observed during an early growth stage (lag-phase), when the growth rate of the cell was slower compared to other stages (Figure 2A-D). *RS-P* in their log-phase resemble dumbbells or elongated dumbbells with beaded structures along its length (Figure 2E-H). Subsequent reduction in the growth rate during stationary phase, transformed *RS-P* into string of beads morphology (Figure 1H & I, 2J-M). Based on these observations, we propose, growth rate as one of the factors regulating the morphology of *RS-P*.

The life cycles (sequential morphological transformation) of *RS-P*, we presented above were consensual rather than a literal. Over multiple reparations, we observed either complete omission of some of a growth stages or cells remained without transforming into another morphology for a prolonged period, which is evident from the presence of all described morphologies in the last growth-stages (Figure 3 & S4). Also, in contrast to our above argument that morphology of *RS-P* is determined by its growth rate (by extension its growth stage), cell morphologies within any given growth stage were seldom uniform and in general are a mix of multiple morphologies (Figure S4 & S8). Length and width of the cells differed considerable from one incubation to an another, even when cultivated under exact same media composition. Moreover, *RS-P* morphologies like large lenticular cells within a filament were not (Figure 3 & S4) reported previously either from lipid vesicles (LV's) or

from living cells. This morphological unpredictability of *RS-P* could be due to a combination of physiology and complex chemical composition of living cells [26].

Morphological unpredictability of *RS-P* could also be explained from a bio-physical prospective. Recent studies attempting to understand similar phenomenon in LV's, suggested that the initial aspect ratio (width: height) of the vesicle determine its end morphology [22,24]. An ever-changing aspect ratio of the vesicles resulted in unpredictable end morphologies. During all growth stages, we observed *RS-P* in a constant state of oscillation (ever changing aspect ratio) (Movie S1), which could also have contributed to the morphological diversity and unpredictability observed in our incubations.

Formation of large lenticular structures (Figure 3) could be explained by anisotropy in physical properties of cell membrane [26]. Biophysical studies focused on understanding morphology and cell replication are mostly a result of studying LV's of rather simpler lipid composition. It was also generally assumed in such studies that the physical properties of LVs like fluidity and elasticity are isotropic along their surface. Unlike LV's, cell membranes have a complex lipid composition and are known to exhibit lateral heterogeneity in their composition and physical properties. It was hypothesized by earlier studies that such differences could result in an un-uniform deformation of membrane surface, leading to the formation of large lenticular structures[26], similar to what was observed in *RS-P*. Together with anisotropy the physical properties, morphological diversity within a given growth stage could also be explained by growth-rate heterogeneity between different cells.

Bacterial growth curves and their partition into different stages (lag, log & stationary) in general represent growth dynamics of bacterial population. Nevertheless, averaging the data

obscure considerable variation in the behavior of individual cells [27,28]. It is known that genetically identical cells within a single bacterial population could exhibit considerable cell-to-cell variation in gene expression [29,30] and their growth rates [31]. Reason for such stochastic behavior of monoclonal cell has to date not been well understood. Manifestation of these variations in the morphology of normal bacteria could not be observed due to the presence of a rigid cell wall, confining cytoplasm of the cell into a pre-determined morphology. Given the absence of a cell wall in *RS-P*, we assume such cell-to-cell variations in growth rate is manifested in its morphology (Figure 2 & S7), which could explain the morphological heterogenicity of cells within any given growth stage.

Different morphologies exhibited by *RS-P* when grown in the KCl and $MgCl_2$ could be due to the nature of interaction between phospholipid membranes and these cations [15]. It is reported that divalent cations like Mg^{+2} organizes lipids into clusters of 10-15 each [32]. This in turn dehydrates and increases the stiffness of the membrane making its area expansion energetically unfavorable. On the other hand, monovalent cations like K^+ are known to reduce bending rigidity of the membrane, making the membrane more flexible [33]. This phenomenon could explain easy expansion of cell membrane, conducive for formation of larger cells.

Earlier studies proposed that fission of a protocells into daughter cells should have been achieved through physical forces. Hence to achieve protocell fission, these studies employed methods like extrusion through a narrow pore size filter or by application of external force [8,34,35]. As most of the cells in the last growth stage are primarily unicellular daughter cells that were formed by fission of filamentous *RS-P* and given the fact that our experiments were conducted under static conditions, we do not assume fission of cells was a result of an

external stimulus. We rather propose that fission of daughter cells was achieved by forces internal to the cell and was a result of internal metabolic reactions [36] or Brownian motion of intracellular constituents[37]. It was also hypothesized that presence of internal metabolism could lead to shape instabilities on the cell surface ultimately leading to cell division [36]. Morphologies and reproductive processes similar to the ones observed in *RS-P* were recently reported among lipid vesicles encapsulating nanoparticles, to emulate Brownian motion of proteins within a cell [37]. Uncanny morphological similarities between morphologies and reproductive processes of *RS-P* with LV's encapsulating nanoparticles from above mentioned study, suggests that morphologies and reproductive processes could have been determined by the physical forces exerted by intracellular constituents. In support of this argument, we observed that cells or intracellular constituents were seldom found in a static state (Movies S2). Such constant movement of cells was a major challenge in imaging cells throughout the study.

Another factor that could have contributed to the fission of cells is the asymmetric conditions on either side of the cell membrane – organic carbon within the cell and inorganic salts outside the cell. Together with the movement of intracellular constituents, such conditions are known to induce constant deformation on the membrane surface. In support of this presumption, addition of bactericidal compounds like sodium azide (0.3%)[38] or formaldehyde[39] did not have any influence on the oscillation of the cells. These oscillations could only be halted when conditions inside and outside the cells were equilibrated by creating pores within the membrane using detergents like Triton X-100 (0.5%), suggesting that asymmetric conditions on either side of the cell membrane contributed to the deformation of cells and provided the force required to mediate cell fission.

Based on the above inferences we argue that fission of parent cell into daughter cells was mediated by physiochemical forces generated by virtue of processing internal metabolism, random movement of cytoplasmic constituents, deformations caused by transient binding of cations to the membrane surface[40] and asymmetric environmental conditions on either side of the cell membrane in terms of osmolarity or nature of the solute [33]. All these conditions are shown to generate shape instabilities, which could have led to fission of cells [36] (Movies S3). Nevertheless, relative contribution of each of these processes to the fission of parent cells is hard to determine in live cells, especially given their metabolic and compositional complexity. Together with the above inferences and reversible morphological transformation of *RS-P* when transferred between media with different salt compositions, suggests that environmental conditions rather than molecular biological processes within the cell determined the morphology and reproductive processes of *RS-P*. Based on our observations we also propose that role of intracellular processes was restricted to harvesting free energy from the surrounding and synthesis of cell constituents rather than regulating cell morphology.

Mechanism of reproduction we observed in *RS-P* was similar to theoretical propositions made for protocell reproduction [8]. In accordance with what was proposed, we observed minimal leakage of cell constituents in *RS-P* (Figure S9). Nevertheless, we assume the efficiency of reproduction was lower in comparison to their original cell state, which is evident from the last growth stage which is characterized by cells that did not underwent cell-division (lenticular cells in Figure 4 & S3) and large quantities of membrane debris (Figure 3C & S4).

Efficiency of reproduction was also dependent on the environmental conditions (Figure S9). Relatively less wastage of cell constituents and production of membrane debris was observed when *RS-P* was grown in the presence of $MgCl_2$ (Figure 4 & S6) than when cultured in DSS or KCl. Reproductive efficiency was also higher when *RS-P* was cultured under non-static conditions (Figure S9). Despite the wastefulness of its reproduction, all our incubations resulted in viable daughter cells with cytoplasmic activity and intracellular DNA (Figure 1, 2, 4, & 7). Subsequent transfer of these cells either directly or after passing through 0.44μm filter to separate daughter cells from other large cells and membrane debris into fresh media always resulted in growth.

In conclusion, our work alters the current presumption that protoplasts reproduce in a haphazard manner. Our observations suggests that in the absence of molecular biological regulatory processes, cells regulate their morphology and reproduce solely based on the physio-chemical properties of their cell constituents. Mechanistically, the morphologies and reproductive processes of these cells can be explained by biophysical properties of cell constituents and environmentally induced phase-separation of cell membrane into L_d and L_o regions i.e., by formation of lateral heterogenicities in membrane lipid composition. Ours is the first study to provide visual evidence for existence of such heterogeneities in living cells, their evolutionary significance and to demonstrate protocell replication in physiologically complex living cells rather than in lipid vesicles. In our subsequent work we were able to demonstrate from the fossil record that this mechanism of reproduction is not merely theoretical, but protocells in-deed reproduced by these processes [41].

Associated content: Supplemental figures; Supplementary movies, Methods and Materials and Supplementary references

Author information: Lead contact, kanaparthi@biochem.mpg.de

Present address: Max-Planck Institute for Biochemistry, Munich, Germany

Notes: The authors declare no competing financial interest.

Author contributions: DK conceived the work with input from TL, BZ, ML & PS. DK performed laboratory experiments. AK did TEM imaging. DK & ML performed confocal super-resolution light microscopy imaging. DK coordinated work between the authors. DK wrote the manuscript with input from TL, BZ, ML, AK & PS. This research was funded by the European Research Council (ERC), grant agreement 616644 (POLLOX) to TL.

Acknowledgments: We gratefully acknowledge Ralf Conrad (Max Planck institute for Terrestrial Microbiology) for his input throughout the work. We would like to thank Gabriella Berthal and Markus Oster for excellent technical support. We would also like to thank Advanced Light Microscopy Facility at EMBL, Heidelberg, Ulf Schwartz from Leica Microsystems, colleagues at Ecological microbiology (Bayreuth University) and cellular biophysics laboratory (Max Planck institute for Biochemistry) and Helmholtz Center Munich for their support throughout the work. We thank Jan-Hagen Krohn for critical reading of the manuscript.

References

(1) Klumpp, S.; Zhang, Z.; Hwa, T. Growth Rate-Dependent Global Effects on Gene Expression in Bacteria. **2009**, *139*, 1366-75.

(2) Adams, D. W.; Errington, J. Bacterial Cell Division: Assembly, Maintenance and Disassembly of the Z Ring. *Nat. Rev. Microbiol.* **2009**, *7*, 642.

(3) Adami, C.; Ofria, C.; Collier, T. C. Evolution of Biological Complexity. *Proc. Natl. Acad. Sci.* **2000**, *97*, 4463–4468.

(4) Carroll, S. B. Chance and Necessity: The Evolution of Morphological Complexity and Diversity. *Nature* **2001**, *409*, 1102-1109.

(5) Faguy, D. M.; Doolittle, W. F. Cytoskeletal Proteins: The Evolution of Cell Division. *Curr. Biol.* **1998**, *8*, R338-R341.

(6) Oparin, A. I. Chemistry and the Origin of Life. *R. Inst. Chem. Rev.* **1969**, *2*, 1-12.

(7) Chen, I. The Emergence of Cells during the Origin of Life. *Science.* **2006**, *314*, 1558-1559.

(8) Zhu, T. F.; Szostak, J. W. Coupled Growth and Division of Model Protocell Membranes. *J. Am. Chem. Soc.* **2009**, *131*, 5705.

(9) Leaver, M.; Dominguez-Cuevas, P.; Coxhead, J. M.; Daniel, R. A.; Errington, J. Life without a Wall or Division Machine in Bacillus Subtilis. *Nature* **2009**, *457*, 849-853.

(10) Wu, L. J.; Lee, S.; Park, S.; Eland, L. E.; Wipat, A.; Holden, S.; Errington, J. Geometric Principles Underlying the Proliferation of a Model Cell System. *Nat. Commun.* **2020**, *11*, 4149.

(11) Blöchliger, E.; Blocher, M.; Walde, P.; Luisi, P. L. Matrix Effect in the Size Distribution of Fatty Acid Vesicles. *J. Phys. Chem. B* **1998**, *102*, 10383–10390.

(12) Knauth, L. P. Salinity History of the Earth's Early Ocean. *Nature* **1998**, *395*, 554.

(13) Blake, R. E.; Chang, S. J.; Lepland, A. Phosphate Oxygen Isotopic Evidence for a

Temperate and Biologically Active Archaean Ocean. *Nature* **2010**, *464*, 1029–1032.

(14) Catling, D. C.; Zahnle, K. J. The Archean Atmosphere. *Sci. Adv.* **2020**, *6*, eaax1420.

(15) Tsai, H. H. G.; Lai, W. X.; Lin, H. Da; Lee, J. Bin; Juang, W. F.; Tseng, W. H. Molecular Dynamics Simulation of Cation-Phospholipid Clustering in Phospholipid Bilayers: Possible Role in Stalk Formation during Membrane Fusion. *Biochim. Biophys. Acta - Biomembr.* **2012**, 1818, 2742-2755.

(16) Kawai, Y.; Mercier, R.; Wu, L. J.; Domínguez-Cuevas, P.; Oshima, T.; Errington, J. Cell Growth of Wall-Free L-Form Bacteria Is Limited by Oxidative Damage. *Curr. Biol.* **2015**, *25*, 1613–1618.

(17) Mercier, R.; Kawai, Y.; Errington, J. Excess Membrane Synthesis Drives a Primitive Mode of Cell Proliferation. *Cell*, **2013**, *152*, 997–1007.

(18) Jülicher, F.; Lipowsky, R. Domain-Induced Budding of Vesicles. *Phys. Rev. Lett.* **1993**, *70*, 2964.

(19) Yanagisawa, M.; Imai, M.; Taniguchi, T. Periodic Modulation of Tubular Vesicles Induced by Phase Separation. *Phys. Rev. E - Stat. Nonlinear, Soft Matter Phys.* **2010**, *82*, 051928-1-9

(20) Yanagisawa, M.; Imai, M.; Taniguchi, T. Shape Deformation of Ternary Vesicles Coupled with Phase Separation. *Phys. Rev. Lett.* **2008**, *100*, 148102-4.

(21) Kato, A.; Tsuji, A.; Yanagisawa, M.; Saeki, D.; Juni, K.; Morimoto, Y.; Yoshikawa, K. Phase Separation on a Phospholipid Membrane Inducing a Characteristic Localization of DNA Accompanied by Its Structural Transition. *J. Phys. Chem. Lett.* **2010**, *23*, 3391–3395.

(22) Zhao, H.; Shaqfeh, E. S. G. The Shape Stability of a Lipid Vesicle in a Uniaxial Extensional Flow. *J. Fluid Mech.* **2013**, *719*, 345-361.

(23) Narsimhan, V.; Spann, A. P.; Shaqfeh, E. S. G. Pearling, Wrinkling, and Buckling of

Vesicles in Elongational Flows. *J. Fluid Mech.* **2015**, *777*, 1–26.

(24) Narsimhan, V.; Spann, A. P.; Shaqfeh, E. S. G. The Mechanism of Shape Instability for a Vesicle in Extensional Flow. *J. Fluid Mech.* **2014**, *750*, 144-190.

(25) Kantsler, V.; Segre, E.; Steinberg, V. Critical Dynamics of Vesicle Stretching Transition in Elongational Flow. *Phys. Rev. Lett.* **2008**, *101*, 048101- 4.

(26) Bobrovska, N.; Góźdź, W.; Kralj-Iglič, V.; Iglič, A. On the Role of Anisotropy of Membrane Components in Formation and Stabilization of Tubular Structures in Multicomponent Membranes. **2013**. *8*, 0073941.

(27) Cooper, S. Distinguishing between Linear and Exponential Cell Growth during the Division Cycle: Single-Cell Studies, Cell-Culture Studies, and the Object of Cell-Cycle Research. *Theoretical Biology and Medical Modelling*. **2006**, *3*, 1-15.

(28) Mitchison, J. M. Single Cell Studies of the Cell Cycle and Some Models. *Theor. Biol. Med. Model.* **2005**, *2*, 1-5.

(29) Kærn, M.; Elston, T. C.; Blake, W. J.; Collins, J. J. Stochasticity in Gene Expression: From Theories to Phenotypes. *Nature Reviews Genetics*. **2005**, *6*, 451-464.

(30) Elowitz, M. B.; Levine, A. J.; Siggia, E. D.; Swain, P. S. Stochastic Gene Expression in a Single Cell. *Science.* **2002**, *297*, 1183-1186.

(31) Strovas, T. J.; Sauter, L. M.; Guo, X.; Lidstrom, M. E. Cell-to-Cell Heterogeneity in Growth Rate and Gene Expression in Methylobacterium Extorquens AM1. *J. Bacteriol.* **2007**, *189*, 7127-7133.

(32) Schultz, Z. D.; Pazos, I. M.; McNeil-Watson, F. K.; Lewis, E. N.; Levin, I. W. Magnesium-Induced Lipid Bilayer Microdomain Reorganizations: Implications for Membrane Fusion. *J. Phys. Chem. B.* **2009**, *113*, 9932-9941.

(33) Karimi, M.; Steinkühler, J.; Roy, D.; Dasgupta, R.; Lipowsky, R.; Dimova, R.

Asymmetric Ionic Conditions Generate Large Membrane Curvatures. *Nano Lett.* **2018**, *18*, 7816-7821.

(34) Deshpande, S.; Spoelstra, W. K.; Van Doorn, M.; Kerssemakers, J.; Dekker, C. Mechanical Division of Cell-Sized Liposomes. *ACS Nano* **2018**, *12*, 2560–2568.

(35) Hanczyc, M. M.; Fujikawa, S. M.; Szostak, J. W. Experimental Models of Primitive Cellular Compartments: Encapsulation, Growth, and Division. *Science.* **2003**, *302*, 618–622.

(36) Zwicker, D.; Seyboldt, R.; Weber, C. A.; Hyman, A. A.; Jülicher, F. Growth and Division of Active Droplets Provides a Model for Protocells. *Nat. Phys.* **2017**, *13*, 408-413.

(37) Vutukuri, H. R.; Hoore, M.; Abaurrea-Velasco, C.; van Buren, L.; Dutto, A.; Auth, T.; Fedosov, D. A.; Gompper, G.; Vermant, J. Active Particles Induce Large Shape Deformations in Giant Lipid Vesicles. *Nature* **2020**, **2020**, *586*, 52-56.

(38) Levy, S.; Chevion, M. Synergistic Cytotoxic Effect of Tetrachlorocatechol and Sodium Azide in Escherichia Coli: Toxicity, Metabolism, and Mechanistic Aspects. *Environ. Toxicol. Chem.* **2009**, *28*, 1380-1389.

(39) Spahn, C.; Grimm, J. B.; Lavis, L. D.; Lampe, M.; Heilemann, M. Whole-Cell, 3D, and Multicolor STED Imaging with Exchangeable Fluorophores. *Nano Lett.* **2019**, *19*, 500-505.

(40) Tarun, O. B.; Okur, H. I.; Rangamani, P.; Roke, S. Transient Domains of Ordered Water Induced by Divalent Ions Lead to Lipid Membrane Curvature Fluctuations. *Commun. Chem.* **2020**, *3*, article number 17.

(41) Kanaparthi, D.; Lampe, M.; Zhu, B.; Boesen, T.; Klingl, A.; Schwille, P.; Lueders, T. On the Nature of the Earliest Known Lifeforms. *bioRxiv* **2021**, 2021.08.16.456462.